Cell Communication & Adhesion, 16, 117–130, 2010
Copyright © 2010 Informa UK, Ltd.
ISSN: 1541-9061 print / 1543-5180 online
DOI: 10.3109/15419060903267539

informa
healthcare

TECHNICAL ADVANCE

Tissue-Specific Cross-Reactivity of Connexin32 Antibodies: Problems and Solutions Unique to the Central Nervous System

Stephanie L. Fowler, Ashleigh C. McLean, and Steffany A. L. Bennett

Neural Regeneration Laboratory and Ottawa Institute of Systems Biology, Department of Biochemistry, Microbiology, and Immunology, University of Ottawa, Ottawa, Ontario, Canada

Cell Commun Adhes Downloaded from informahealthcare.com by University of Ottawa on 12/27/10
For personal use only.

Abstract

Gap junction proteins are a highly homologous family of 21 connexins. Here, the authors describe a tissue-specific technical artifact complicating analysis of connexin32 protein expression in the central nervous system. The authors show that in brain, but not liver, eight commonly employed antibodies exhibit a higher affinity for a cross-reactive protein that masks the detection of connexin32. Cross-reactivity is evident in Western blot analyses when proteins are subjected to reducing/denaturing conditions but not immunoprecipitation or in situ immunofluorescent applications. Through bioinformatic analyses, tested by sucrose gradient fractionation and immunoblotting of lysates from connexin null-mutant mice, the authors show that the cross-reactive protein is not found in the same cellular compartments as connexin32 and is likely not a member of the connexin family. These findings are presented with the intent of helping to reduce the amount of time laboratories currently expend in validating changes in connexin32 expression in the central nervous system.

Keywords: brain, connexin32, cross-reactivity, gap junction, immunoblotting, liver

INTRODUCTION

Connexin proteins are a highly conserved family of single- and double-membrane channels characterized, in part, by four transmembrane-spanning domains. The connexin family consists of 21 members, 11 of which are expressed in the mammalian central nervous system (CNS) (Rouach et al. 2002; Nakase and Naus 2004; Sohl et al. 2005). Hexamerization of compatible connexins form structures called connexons that incorporate as hemichannels in nonjunctional membranes (single-membrane channels) or dock with compatible connexons donated from adjacent cells to form intercellular gap junction channels (double-membrane channels) (Goodenough and Paul 2003). Gap junctions are present in membranes as plaques composed of hundreds of channels of various connexin combinations that allow for the transfer of ions and metabolites less than 1 kDa in size between neighboring cells (Bruzzone et al. 1996).

Connexin32 (Cx32) is the predominant liver connexin, and was first isolated in 1986 from purified calf liver gap junctional preparations (Paul 1986). Hydropathy analysis of the Cx32 cDNA clone predicted a protein with four transmembrane domains flanked by α-helical loops. Shortly thereafter, the cytoplasmic localization of both N- and C-termini, and a hydrophilic domain corresponding to the loop between the second and third transmembrane regions, were confirmed (Figure 1). It is generally accepted that these cytoplasmic regions are the least conserved amongst connexin family members, and thus provide the most attractive sites for connexin-specific antibody development (Hertzberg 1985; Goodenough et al. 1988).

The first Cx32 antibodies were prepared from purified calf liver gap junction preparations (Traub et al. 1982; Paul 1986) or from peptides localized to the C-terminus, and the intracellular loop (Hertzberg 1985; Goodenough et al. 1988). Each of these antibodies recognized a monomeric protein with a molecular weight of approximately 27 kDa, as well as the predicted Cx32 dimer migrating at approximately 54 kDa. Specificity was confirmed by peptide competition and by qualitative observations of target protein oligomerization upon heating in sodium dodecyl sulfate (SDS), a defining characteristic of connexin proteins (Hertzberg 1985; Goodenough et al. 1988). However, the ultimate

Received 20 June 2009; accepted 18 August 2009

Stephanie L. Fowler and Ashleigh C. McLean contributed equally to this work.

The authors wish to thank Jean-Philippe Lambert and Daniel Figeys (Ottawa Institute of Systems Biology) for their ingenuity and technical expertise and Dr. Jim Nagy (University of Manitoba) for critical reading of the manuscript and helpful suggestions as to how to further improve immunofluorescent detection of Cx32 in situ. This work was supported by an operating grant (MOP62826) and salary support from the Canadian Institute of Health Research (CIHR) to S.A.L.B. S.F. was supported by an Ontario Graduate Studentship. A.C.M. received a travel award from the CIHR Institute of Gender and Health in support of these studies.

Address correspondence to: Dr. Steffany Bennett, Neural Regeneration Laboratory and Ottawa Institute of Systems Biology, Department of Biochemistry, Microbiology, and Immunology, 451 Smyth Road, Ottawa, ON, Canada, K1H 8M5. Tel: (613) 562-5800×8372; Fax (613) 562-5452; E-mail: sbennet@uottawa.ca

RIGHTSLINK

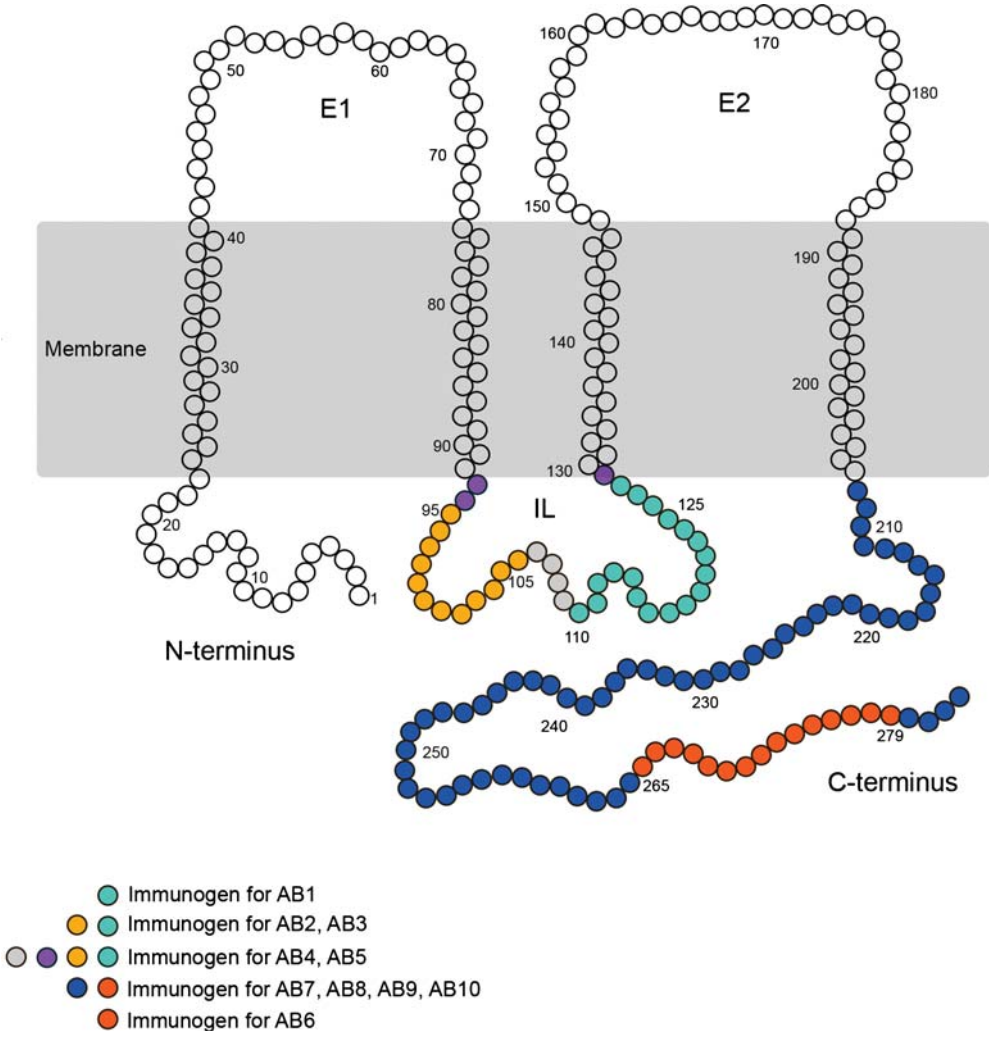

Figure 1. Schematic of the transmembrane structure of Cx32, highlighting the position of the peptides used to generate each of the antibodies assessed. Additional details are provided in Table 1.

negative control for any immunogenic protein analysis lies in analysis of samples from a null-mutant animal. The Cx32 null-mutant mouse, generated by the Willecke laboratory, has greatly facilitated the investigation of Cx32 localization and function (Nelles et al. 1996). This control has confirmed that Cx32 is predominantly expressed in myelinating glia (oligodendrocytes and Schwann cells) of the CNS and peripheral nervous system (Scherer et al. 1995; Dermietzel et al. 1997; Li et al. 1997; Altevogt et al. 2002; Melanson-Drapeau et al. 2003; Nagy et al. 2003a).

Although great care has been taken to ensure antibody specificity in tissues with high levels of target connexin expression (i.e., specific detection of Cx32 in liver, Cx45 in heart), few studies have assessed the potential for cross-reactivity in the CNS wherein an extensive repertoire of connexins is expressed in different cell types (Traub and Willecke 1982; Nagy et al. 2003b). Unpublished data from our laboratory and anecdotal reports from other groups have detected a 27- to 32-kDa anti-Cx32 reactive band in murine brain and spinal cord homogenates of Cx32-null animals by Western blot analysis using antibodies that have been repeatedly verified for appropriate immunofluorescent analyses (Melanson-Drapeau et al. 2003; Nagy et al. 2003a, 2004). Because laboratories are understandably reticent to publish the appearance of spurious artifacts, these observations have not been systematically evaluated; however, the presence of a cross-reactive band, with the same approximate mobility in null-mutant animals, represents an important complication in the analysis of Cx32 by Western analysis following CNS injury.

To address this issue, we compared reactivity of 10 commonly used Cx32 antibodies in brain and liver using immunoblotting, immunofluorescence, and immunoprecipitation applications. Surprisingly, we found that eight antibodies cross-reacted with a protein present in $Cx32^{Y/-}$ brain but not liver. We show that this cross-reactivity is only observed when proteins were subjected to reducing/denaturing conditions prior to immunodetection. To further distinguish Cx32 from CNS-specific cross-reactive protein(s), we used using sucrose gradient fractionation, demonstrating that Cx32 and the cross-reactive protein(s) localize to distinct subcel-

Cell Commun Adhes Downloaded from informahealthcare.com by University of Ottawa on 12/27/10
For personal use only.

RIGHTSLINK

Table 1. Connexin antibodies

Code	Catalogue number	Source	Epitope location[a]	Type[b]	[Western]	[Immuno]
AB1	CX32C13-M	Alpha Diagnostics	IL 110-128	Monoclonal	0.5 µg/ml	1:200
AB2	Hybridoma	David Paul	IL 95-125	Monoclonal	No dilution	No dilution
AB3	MAB3069	Chemicon	IL 95-125	Monoclonal	1:1000	1:100
AB4	13-8200	Zymed	IL[c]	Monoclonal	1:250	1.0 µg/ml
AB5	71-0600	Zymed	IL[c]	Polyclonal	1:125	2.0 µg/ml
AB6	C3470	Sigma	C-term 265-279	Polyclonal	1:200	1:600
AB7	C7854-05E	USBiological	C-term 19 aa	Polyclonal	0.7 µg/ml	1:400
AB8	C7854-04	USBiological	C-term	Polyclonal	3.0 µg/ml	1:800
AB9	34-5700	Zymed	C-term[d]	Polyclonal	1:125	1.0 µg/ml
AB10	35-8900	Zymed	C-term[d]	Monoclonal	3.0 µg/ml	1:800
AB11	51-2800 (Cx26)	Zymed	C-term	Polyclonal	1:125	NA
AB12	71-2200 (Cx30)	Zymed	C-term	Polyclonal	1:200	NA

NA, not applicable.
[a]Peptides used to generate each antibody are listed by amino acid position where known (see Figure 1). Position and/or length of the peptides used to generate AB4, AB5, AB7-10 were not disclosed by the manufacturer. IL, intracellular loop; C-term, C-terminus.
[b]All monoclonal antibodies were raised in mouse. All polyclonal antibodies were raised in rabbit.
[c]AB4 and AB5 were raised against the same proprietary IL antigen.
[d]AB9 and AB10 were raised against the same proprietary C-term antigen.

Cell Commun Adhes Downloaded from informahealthcare.com by University of Ottawa on 12/27/10
For personal use only.

lular compartments and exhibit a 4-kDa size difference. Finally, combined bioinformatics and molecular approaches provide converging evidence that the cross-reactive protein is likely not another connexin but rather an immature (Golgi-localized) or partially degraded (lysosome-localized) subunit of a larger unidentified protein complex. Together, these data highlight a key concern for the interpretation of changes in Cx32 protein expression in the CNS that can be easily controlled by the choice of methodology and the optimized reagents described in this study.

MATERIALS AND METHODS

Cx32 Antibodies

Table 1 describes the Cx32 antibodies employed, the peptides used to generate each antibody, the antigenic sites within these peptide sequences, the source of each antibody, and the concentrations employed.

$Cx32^{Y/+}$ and $Cx32^{Y/-}$ Animals

Cx32 null-mutant breeding pairs (Nelles et al. 1996), kindly provided by Dr. Klaus Willecke (Universitat Bonn, Germany), were backcrossed for 13 generations onto a C57Bl/6 background in our laboratory. Congenic wild-type mice were derived from heterozygote matings. Male mice used in this study were 3 to 4 months of age at the time of sacrifice. A total of 15 $Cx32^{Y/+}$ and 15 $Cx32^{Y/-}$ mice were analyzed. Genotyping was confirmed at time of weaning and again at time of sacrifice (Supplemental Figure 1). DNA isolated from tail snips was amplified using primers A, B, and C (A: 5′-TCA TTC TGC TTG TAT TCA GGT GAG AGG CGG-3′; B: 5′-ATA CAC CTT GCT CAG TGG CGT GAA TCG GCA-3′; C: 5′-TCT TAC TCC ACA CAG GCA TAG AGT GTC TGC-3′). A and B amplified a 750-bp fragment of the $Cx32^{Y/+}$ wild-type (WT) allele, whereas A and C produced a 1.3-kb fragment indicating the $Cx32^{Y/-}$ knockout (KO) allele (Supplemental Figure 1). Polymerase chain reaction (PCR) amplification was performed on a Whatman Biometra TGradient96 system. Cycling parameters were 95°C for 10 min, followed by 30 cycles of 95°C for 60 s, 67°C for 60 s, and 72°C for 60 s.

Immunoblotting

Brain tissue (encompassing either cerebrum and cerebellum or dissected hippocampus as indicated) was isolated from $Cx32^{Y/+}$, $Cx32^{Y/-}$, $Cx32^{Y/-}Cx29^{-/-}$, and $Cx30^{-/-}$ mice. $Cx29^{-/-}$ mice (Altevogt et al. 2002) were kindly provided by Dr. David Paul (Harvard Medical School) and crossed onto a Cx32 null-mutant background in our laboratory. $Cx30^{-/-}$ breeding pairs (Teubner et al. 2003) were obtained through the European Mouse Mutant Archive with the kind assistance of Dr. Klaus Willecke. Liver was obtained from the same animals. Human brain from a 67-year-old female who suffered sudden death due to non-neurological complications was obtained from the Douglas Hospital Research Centre Brain Bank (Montreal, Canada). At autopsy, parahippocampal gyri were removed and flash-frozen in liquid nitrogen without fixation for protein extraction. Postmortem delay was 17 h. The hippocampus was dissected from this sample for Western analysis. All tissues were homogenized in fresh RIPA buffer (1% Nonidet P-40, 0.5% sodium deoxycholate, 0.1% SDS, 1 mM NaF, 50 g/ml aprotinin, 1 mM sodium orthovanadate, 1 mg/ml phenylmethylsulfonyl fluoride, 10 mM phosphate-buffered saline [PBS; 10 mM phosphate, 154 mM NaCl]) and assayed for protein concentration using a Bio-Rad DC protein

RIGHTSLINK

Cell Commun Adhes Downloaded from informahealthcare.com by University of Ottawa on 12/27/10
For personal use only.

assay kit (Bio-Rad, Hercules, CA). Brain and liver samples were diluted in 2 × SDS sample buffer (Tris-HCl/SDS pH 6.8, 5% glycerol, 1.67% SDS, 100 mM dithiothreitol, 0.002% bromophenol blue) with 10% β-mercaptoethanol (BME) and solubilized at room temperature for 30 min. All experiments were performed and repeated using 30 µg of hippocampal or whole-brain protein and 10 µg of liver protein to allow for comparable signal and exposure times given the differences in abundance of Cx32 protein between liver and brain tissue. Proteins were resolved under reducing/denaturing conditions on 12.5% or 15% (sucrose fractions only) Tris-HCl polyacrylamide gels and transferred onto Immobilon P^{SQ} polyvinylidene fluoride (PVDF) membrane (Millipore, MA) at 100 V for 60 min. Membranes were blocked in 5% (*w/v)* skim milk powder–PBS with 0.1% Tween-20 (PBST; blocking buffer) for 1 to 3 h and incubated in primary antibody diluted in the same buffer overnight at 4°C (see Table 1 for working concentrations of all connexin antibodies). Membranes were rinsed twice in 0.1% PBST and twice in blocking buffer for 10 min prior to a 1- to 3-h incubation in horseradish peroxidase (HRP)-conjugated anti-mouse or anti-rabbit (Jackson ImmunoResearch Laboratories, PA; 1:2000 and 1:5000) secondary antibody diluted in blocking buffer. Signal was detected on x-ray film using SuperSignal West Pico Chemiluminescent Substrate (Pierce, IL).

Immunofluorescence

Male mice ($Cx32^{Y/+}$ and $Cx32^{Y/-}$) were anesthetized with Euthansol (65 mg/ml) and intracardially perfused with 10 mM PBS (pH 7.2) followed by 3.7% molecular grade paraformaldehyde (Sigma) in 10 mM PBS diluted immediately prior to use. Brain and liver were removed and postfixed for 24 h at 4°C in the same fixative followed by 48 h of cryoprotection in 20% sucrose solution containing 0.001% sodium azide at 4°C. Serial cryostat sections (10 µm) were obtained (Leica Microsystems). Sections were immunoreacted with anti-Cx32 primary antibodies (Table 1) diluted in antibody buffer (10 mM PBS, 0.3% Triton-X100, 3% bovine serum albumin [BSA]). Optimal concentrations were determined by serial dilution on both liver and brain sections with the antibody concentration giving the most robust signal employed for the rest of the study. Where antibodies were not reactive or showed cross-reactivity on brain tissue, the optimal concentration determined using liver cryosections was employed. Secondary antibodies used were Cy3- or fluorescein isothiocyanate (FITC)-conjugated anti-mouse immunoglobulin G (IgG) (diluted 1:800 and 1:400, respectively) and Cy3- or FITC-conjugated anti-rabbit IgG (1:600, 1:100; Jackson ImmunoResearch Laboratories, PA). Details are as described in Melanson-Drapeau et al. (2003). Sections were coverslipped in 0.05% *p*-phenylenediamine in PBS/glycerol, pH 8.0, and imaged by epifluorescent microscopy using OpenLab 5.0.2 (Improvision) on a DMXRA2 epifluorescent microscope (Leica Microsystems).

Immunoprecipitation

Cx32-coupled protein G agarose beads were prepared as follows: One milliliter of protein G agarose bead slurry (1:1 PBS; Roche, Germany) was incubated with 25 µg of AB1 (Table 1) overnight at 4°C. The beads were washed with 10 ml of 0.1 M borate buffer (pH 9.0) and resuspended in 10 ml of the same buffer. AB1 was chemically coupled to the protein G beads by the addition of solid dimethylpimelimidate (Pierce, IL) to a final concentration of 20 mM. Beads were incubated for 30 min at room temperature. The reaction was stopped by washing the beads twice with 0.2 M ethanolamine. Beads were resuspended in 10 ml of 0.2 M ethanolamine and incubated at room temperature for 2 h, followed by two washes with 10 ml of PBS. Beads were resuspended in 1 ml PBS and stored at 4°C.

Human and mouse hippocampal and brain lysates as well as mouse liver lysates were prepared for Western analyses in RIPA buffer with fresh protease inhibitors and assayed for protein concentration. Protein lysates were diluted to 100 µg in 200-µl volumes for preclearing with 50 µl of uncoupled protein G agarose beads for 1 h at 4°C. Precleared lysates were added to 50 µl of prepared AB1-coupled beads and incubated overnight at 4°C. Beads were washed twice in RIPA buffer and three times in PBS. Proteins were eluted from the IgG molecules at room temperature for 30 min with inversion in 200 µl of ammonium hydroxide elution buffer (0.5 M NH_4OH, 0.5 mM EDTA). Samples were lyophilized in a SpeedVac and solubilized in 45 µl 2 × SDS sample buffer and 5 µl BME at room temperature for 30 min. The SDS-solubilized proteins were resolved on 12.5% Tris-HCl polyacrylamide gels, transferred to PDVF membranes, and blotted with polyclonal AB6.

Sucrose Gradient Fractionation

Whole brain and whole liver were extracted from $Cx32^{Y/+}$ and $Cx32^{Y/-}$ mice and immediately frozen in liquid nitrogen. For each experiment, one brain hemisphere or one lobe of liver was homogenized in 1.5 ml PTN buffer (50 mM sodium phosphate, 1% Triton X-100, 50 mM NaCl, 30 µl protease inhibitor cocktail, pH 7.4) using a Teflon Potter-Elvehjem homogenizer fitted to a 30-ml glass tube. Homogenates were incubated on ice for 30 min and centrifuged at 16,000 × *g* for 10 min at 4°C. The Triton X-100 soluble supernatant was reserved on ice. One milliliter of supernatant was mixed with 1 ml 80% sucrose. Samples were carefully overlaid with 1.5 ml 30% sucrose followed by 1.5 ml of 5% sucrose. Prepared tubes were centrifuged at 130,000 × *g* in an SW-40 Ti swinging-bucket rotor overnight (18 h) at 4°C (Beckman 50 Ultra-Clear Tubes [14 × 95 mm]; catalog number 344060). Gradients were carefully aliquoted (10 fractions at 500 µl each), with fraction 1 being the uppermost, lightest fraction. Protein quantification was performed using the Bio-Rad DC protein assay kit, and samples were

RIGHTSLINK

analyzed by immunoblotting using AB1 and the fractionation markers coxIV (Molecular Probes [A-21348] 0.4 μg/ml), caveolin-1 (Santa Cruz [SC-894] 1:500), flotillin-1 (BD Transduction Laboratories [610820] 1:1000), syntaxin-1 (Sigma [S0664] 1:2000), LAMP1 (Cell Signaling [C54H11] 1:1000), and golgin-97 (Molecular Probes [A-21270] 1:1000).

Mass Spectrometric Identification of Proteins after Western Analysis

Blotting and removal of nitrocellulose (BARN) methodology followed by tryptic digest and mass spectrometry analysis were performed as described in Luque-Garcia et al. (2008) to identify the Cx32 cross-reactive protein under reducing/denaturing conditions. Briefly, 20 μg of liver fractions 4, 5, and 6 from a $Cx32^{Y/+}$ fractionation were resolved in each of eight lanes of a 12.5% sodium dodecyl sulfate–polyacrylamide gel electrophoresis (SDS-PAGE) gel and transferred to a nitrocellulose membrane (Triton-free, pore size 0.2 μm) at 400 mA for 1 h on ice in transfer buffer (25 mM Tris, 192 mM glycine, 0.1% SDS, 20% methanol). The membrane was blocked with PVP-40 buffer (0.5% *w/v* poly(vinylpyrrolidone) in 100 mM acetic acid) for 1 h at room temperature and rinsed with four changes of PBS (1 min each) before overnight incubation with AB1 diluted in PBS. Primary antibody was rinsed from the membrane with four changes of PBS (10 min each), incubated with anti-mouse IgG-HRP secondary antibody diluted in PBS for 1 h, followed by four rinses in PVP-40 blocking buffer. The membrane was rinsed with four changes of PBS (1 min each) to remove excess PVP-40 buffer. Chemiluminescent detection was performed as usual except that all surfaces coming into contact with the membrane were washed with 70% ethanol and rinsed with double-distilled H_2O (ddH_2O) to prevent keratin contamination. The developed film was aligned with the chemiluminescent stain on the membrane to facilitate accurate detection of the Cx32-containing region of the membrane. Each of the eight Cx32-containing bands were excised with no. 11 scalpel blades and washed three times with 1.5 mL 20 mM sodium bicarbonate buffer (pH 7.4) for 5 min each at room temperature. The membrane sections were then washed three times with 1.5 ml 100 mM glycine (pH 2.4) for 10 min to remove all traces of antibody before a final 5-min wash in 1.5 ml 20 mM sodium bicarbonate buffer. The nonspecific sites on the membrane sections were blocked with 0.5 ml PVP-40 buffer for 30 min at 37°C and rinsed six times with ddH_2O. Trypsin (Promega) prepared in 50 mM NH_4HCO_3 buffer (pH 8) was added at 12.5 ng/μl to the membrane sections and incubated at 37°C overnight. The samples were dried under vacuum and dissolved by vortexing in acetone (90 μl acetone/4 mm^2 nitrocellulose) followed by a 30-min incubation at room temperature. The acetone containing the nitrocellulose was removed, and the peptides were air-dried and resuspended in 20 μl 2% acetonitrile in 0.1% formic acid. Nanoflow liquid chromatography tandem mass spectrometry (LC-MS/MS) was used to analyze peptide mixtures derived from these on-membrane digestions as described by (Luque-Garcia et al. 2008) and data were analyzed as in Lambert et al. (2009).

RESULTS

A Cross-Reactive Protein with the Same Mobility as Cx32 Is Detected in Null-Mutant Brain But Not Liver

Protein lysates prepared from murine tissue (liver, brain, and isolated hippocampus) as well as human hippocampus were resolved by SDS-PAGE under reducing conditions. Western analysis was performed using 10 different Cx32 antibodies (Table 1, Figure 1). Five antibodies were directed against epitopes localizing to the intracellular loop (Figures 1, 2); five antibodies were directed against epitopes found within the C-terminal tail of Cx32 (Figures 1, 3). Because six of the antibodies tested were raised against proprietary peptide sequences (Table 1), three algorithms (Hopp and Woods 1981; Kyte and Doolittle 1982; Kolaskar and Tongaonkar 1990) were used to identify the peptides most likely to raise an immunogenic response within the targeted region using (1) Antigenic Peptide Tool (Immunomedicine group at Universidad Complutense de Madrid; Kolaskar and Tongaonkar method) and (2) Abie Pro 3.0 (Chang Biosciences; Hopp-Woods and Kyte-Doolittle hydrophillicities). For each prediction tool, the peptide size was set to 8. Results are presented in Table 2 and mapped in Figures 2 and 3.

In immunoblots of rat liver lysates, Cx32 migrates with a mobility of approximately 27 kDa under reducing/denaturing conditions (Paul 1986). As expected, this same pattern was detected in murine liver (Figures 2, 3, Liver). All of the antibodies tested reacted specifically with a protein migrating just below the 31-kDa protein standard that was absent from the $Cx32^{Y/-}$ controls (Figures 2, 3, Liver, *closed arrowhead)*. However, in lysates prepared from either whole brain or dissected hippocampus, seven of the antibodies (AB1 to AB4, AB6, AB8, AB9) detected a cross-reactive protein(s) with the same mobility as Cx32 in both $Cx32^{Y/+}$ and $Cx32^{Y/-}$ samples (Figures 2A to D, 3A, C, D, *arrow)*. Some species variation in reactivity was also observed. AB4 (Figure 2D, *open arrowhead)*, AB8 (Figure 3C, *open arrowhead)*, and AB9 (Figure 3D, *open arrowhead)* detected a doublet in human hippocampus, but only one species in murine brain/hippocampus. However, this single species was also evident in $Cx32^{Y/-}$ samples (Figures 2D, 3C, D, *arrow)*. AB7 detected a doublet that migrated above the 31-kDa marker in all murine CNS samples (Figure 3B, *open arrow)* but failed to react with human protein (Figure 3B).

Only AB5 and AB10 detected Cx32 specifically in brain tissue (Figures 2E, 3E *closed arrowhead)*. Some species variations were again observed in that the human

Cell Commun Adhes Downloaded from informahealthcare.com by University of Ottawa on 12/27/10
For personal use only.

RIGHTSLINK

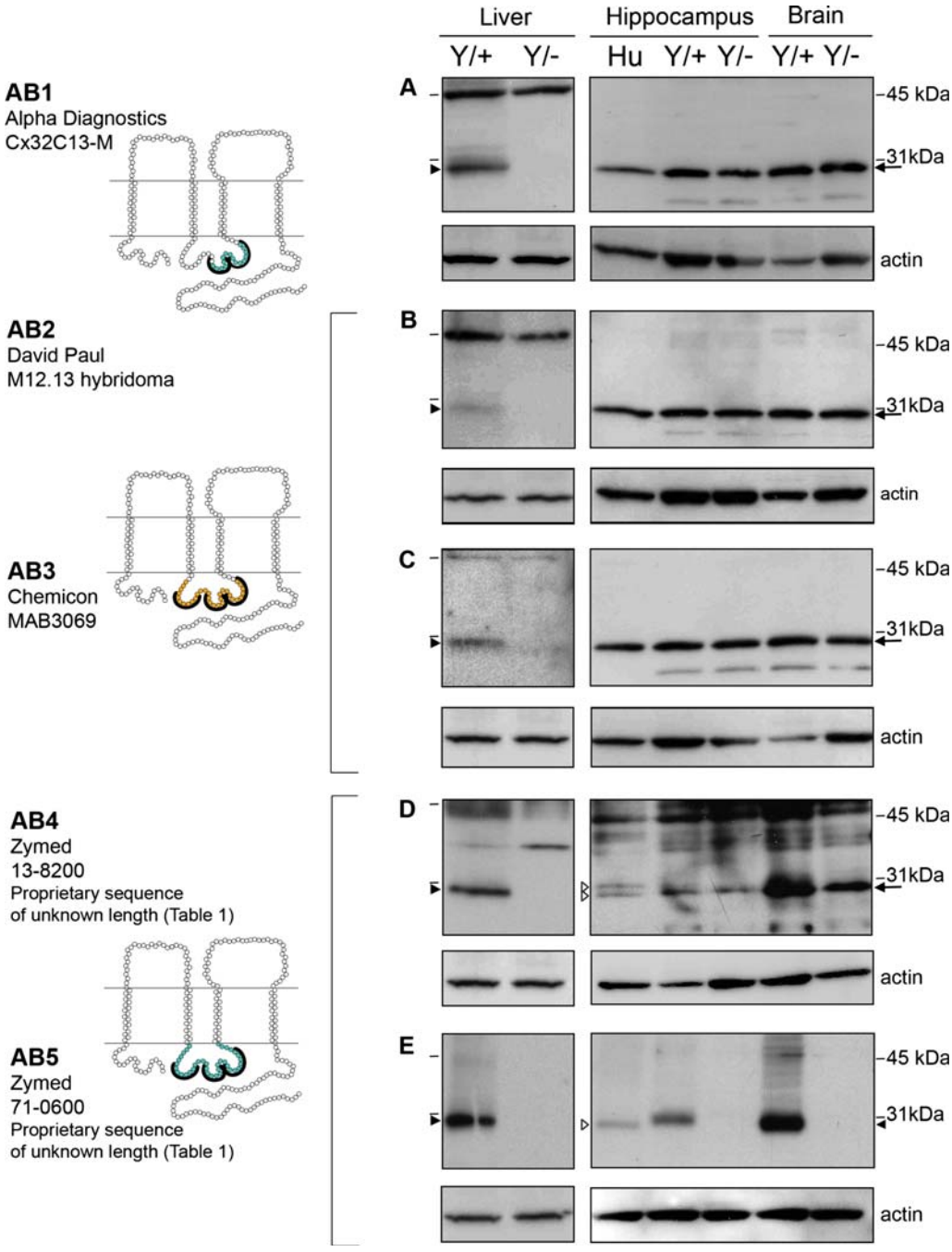

Figure 2. Four of the five Cx32 antibodies directed against the intracellular loop cross-react with a protein exhibiting the same mobility as Cx32 in $Cx32^{Y/-}$ brain but not $Cx32^{Y/-}$ liver under reducing/denaturing conditions. **(A–E,** *left panel***)** Transmembrane schematics of the peptides for each Cx32 antibody, with the colored circles representing available information about each immunizing peptide sequence. Black brackets indicate primary sequence with the highest antigenic potential (see Table 2). **(A–E,** *right panel***)** Cx32 immunoblots were performed using 10 µg liver or 30 µg of human (Hu) and murine hippocampus or brain lysates. Lines indicate size markers. Black arrowheads point to Cx32 specifically detected by all antibodies in liver **(A–E)** and AB5 in brain **(E)**. White arrowheads indicate isoform variations specific to human samples **(D, E)**. Arrows indicate the cross-reactive protein(s) detected by AB1 to AB4 in both $Cx32^{Y/+}$ brain tissue and the $Cx32^{Y/-}$ control **(A–D)**. Note that this particular cross-reactive protein(s) migrates with the same mobility as Cx32 when separated on 12.5% Tris-HCl polyacrylamide gels.

protein appeared to migrate faster than murine Cx32 in hippocampal lysates (Figure 2E, *open arrowhead)*, possibly as a doublet (Figure 3E, *open arrowheads)*. The Cx32-specific signal detected using AB5 and AB10 was more abundant in lysates prepared from whole brain (and thus enriched in protein isolated from myelinated fiber tracts containing Cx32-expressing oligodendrocytes) than in hippocampal lysates (Figures 2E, 3E, compare murine brain to hippocampus). This expression pattern is consistent with the expected localization of Cx32. Conversely, the signal intensity of the cross-reactive protein was comparable across samples (Figures 2A to D, 3A to D, *arrow)*.

Cell Commun Adhes Downloaded from informahealthcare.com by University of Ottawa on 12/27/10
For personal use only.

RIGHTSLINK

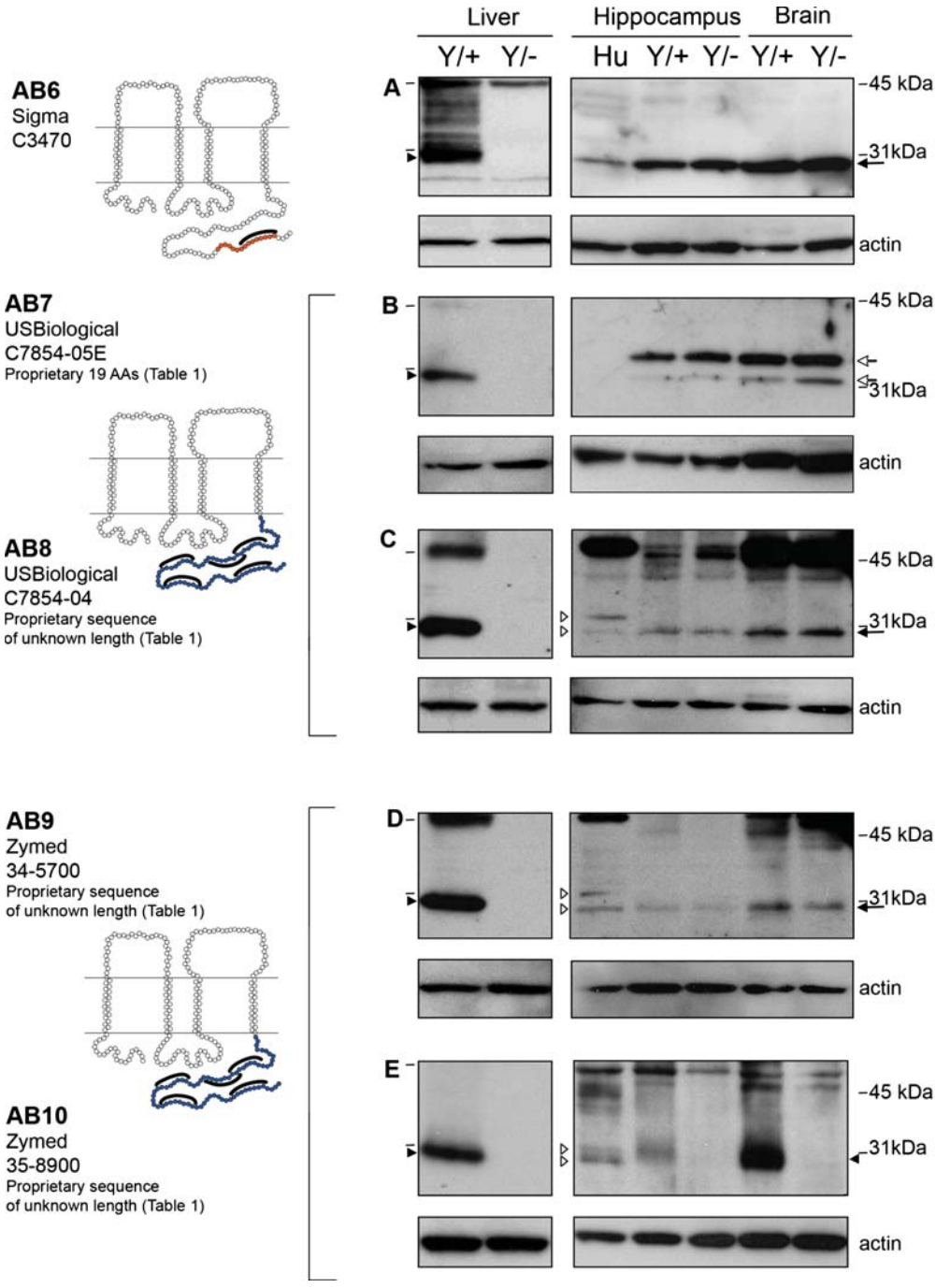

Figure 3. Four of the five Cx32 antibodies directed against the C-terminal tail cross-react with a protein exhibiting the same mobility as Cx32 in $Cx32^{Y/-}$ brain but not $Cx32^{Y/-}$ liver under reducing/denaturing conditions. As in Figure 2, lines indicate size markers. Closed arrowheads point to Cx32 specifically detected by all antibodies in liver **(A–E)** and AB10 in brain **(E)**. White arrowheads indicate isoform variations specific to human samples **(C–E)**. Arrows indicate the cross-reactive protein(s) detected by AB6-9 in both $Cx32^{Y/+}$ brain tissue and the $Cx32^{Y/-}$ control **(A–D)**. Note that this particular cross-reactive protein(s) migrates with the same mobility as Cx32 when separated on 12.5% Tris-HCl polyacrylamide gels. All other details are as in Figure 2.

Cx32 Immunofluorescent Analysis Is Not Confounded by Cross-Reactivity with Other Proteins in Murine Brain

To test whether this tissue-specific cross-reactivity is also detected in situ, immunofluorescent analysis of fixed 10-μm liver and brain cryosections was performed. As expected, all 10 of the antibodies detected Cx32 at hepatocyte plasma membrane in $Cx32^{Y/+}$ liver tissue, with minimal to no background reactivity in the $Cx32^{Y/-}$ controls (Figures 4A to E, 5A to E, Liver, *arrows)* with the exception of low level labeling of rare heptatocyte

Cell Commun Adhes Downloaded from informahealthcare.com by University of Ottawa on 12/27/10
For personal use only.

RIGHTSLINK

Table 2. Antigenic sites along the IL and C-terminus of the Cx32 protein

	Site (amino acid position)[a]	Sequence	Hopp-Woods	Kyte-Doolittle	Kolaskar and Tongaonkar
IL epitopes	118-125	EEVKRHKV	✓	✓	
	98-105	QQHIEKKM	✓	✓	
	109-116 (112-119)	EGHGDPLH	✓	✓	✓ (GDPLHLEE)
C-term epitopes	220-227	AQRRSNPP	✓	✓	
	225-232	NPPSRKGS	✓	✓	
	239-246 (235-242)	SPEYKQNE	✓	✓	✓ (FGHRL SPE)
	252-259	SEQDGSLK	✓	✓	
	271-278	GLAEKSDR	✓	✓	

Abbreviations are as in Table 1.
[a]Sites are listed from most to least likely to raise an antibody response determined using three different bioinformatic tools: (1) Antigenic Peptide Tool (Immunomedicine group at Universidad Complutense de Madrid; Kolaskar and Tongaonkar method); (2) Abie Pro 3.0 (Chang Biosciences; Hopp-Woods and Kyte-Doolittle hydrophilicities).

Cell Commun Adhes Downloaded from informahealthcare.com by University of Ottawa on 12/27/10
For personal use only.

membranes with AB5 (Figure 5E, Liver, *arrowhead)*. Some of the antibodies detected intracellular pools of Cx32 in addition to robust immunostaining at the membrane (AB2, AB7, and AB9) (Figures 4B, 5B, D, Liver).

None of the antibodies exhibited significant cross-reactivity with $Cx32^{Y/-}$ brain tissue (Figures 4A to E, 5A to E, $Cx32^{Y/-}$ hippocampus), with the possible exception of AB6 at the highest concentration tested (Figure 5A). Each reagent was examined over a minimum of three concentrations. The dilution that gave optimal signal in brain sections is presented in Figure 4 and Table 1. Where specific signal was not detected in hippocampus (Figures 4C, 5) or corpus callosum (not shown), the dilution optimal for detection of Cx32 in liver sections is shown (Table 1, Figures 4, 5). Four of 10 antibodies tested (AB1, AB2, AB4, and AB5) reliably detected fixed protein in situ in mouse hippocampal sections (Figure 4A, B, D, E $Cx32^{Y/+}$ hippocampus) under the perfusion, postfixation, and cryoprotection protocol employed here, with AB4 providing the most robust signal (Figure 4D). All of these antibodies were directed against epitopes localizing to the intracellular loop of Cx32. Immunostaining was evident at the plasma membrane of cells with the expected oligodendrocyte and/or oligodendrocyte precursor cell morphology (Figures 4A, B, D, E $Cx32^{Y/+}$ hippocampus). None of the C-terminal–directed antibodies produced a specific immunosignal under the fixation protocol defined in Materials and Methods (Figure 5A to E, $Cx32^{Y/+}$ hippocampus). Moreover, AB6 exhibited some artifactual labeling of neurons in both $Cx32^{Y/+}$ and $Cx32^{Y/-}$ sections Figure 5A, compare labeling in the granular layer of the Dentate Gyrus, GrDG.

Cross-Reactivity Is Not Observed When Tertiary Structure Is Maintained during Initial Detection

Taken together, these results suggested that cross-reactivity is primarily detected in CNS tissue under denaturing/reducing conditions. These data led us to hypothesize that antibody cross-reactivity was dependent upon protein conformation. To test this hypothesis, the tertiary conformation of Cx32 was maintained during immunoprecipitation before being subjected to denaturing/reducing conditions in immunoblot detection. This approach restored specific detection of Cx32 in brain tissue (Figure 6A, Hippocampus and Brain, *arrow)*. No cross-reactivity was observed in $Cx32^{Y/-}$ samples (Figure 6A). Mobility was consistent with that observed in liver lysate controls subjected to Western blotting only (Figure 6A, Liver, *arrow)*. To further confirm that this specificity was conformation dependent, aliquots of the same protein samples used in the immunoprecipitations (Figure 6A) were analyzed by Western blotting (Figure 6B). Figure 6B reiterates the presence of a cross-reactive species in $Cx32^{Y/-}$ brain lysates immunoblotted under reducing/denaturing conditions.

The Brain-Specific Cross-Reactive Protein(s) Is Expressed at Higher Levels Than Endogenous Cx32 and Exhibits a Distinct Subcellular Localization

Although demonstrating that Cx32 can be detected specifically in brain tissue by immunoprecipitation, this finding also limited our capacity to identify cross-reactive CNS protein(s) by standard proteomic protocols. As an alternative, we attempted BARN to identify proteins present in the anti-Cx32–immunoreactive bands under reducing/denaturing conditions (Luque-Garcia et al. 2008). We were, however, unable to detect Cx32 from on-membrane digestions of $Cx32^{Y/+}$ liver samples despite successful identification of other co-migrating proteins (data not shown). As such, we lacked the appropriate positive control required to apply this profiling approach to identify the anti-Cx32–reactive proteins in $Cx32^{Y/+}$ and $Cx32^{Y/-}$ brain samples.

We turned to an analysis of AB1-reactive proteins under denaturing/reducing conditions using sucrose

RIGHTSLINK

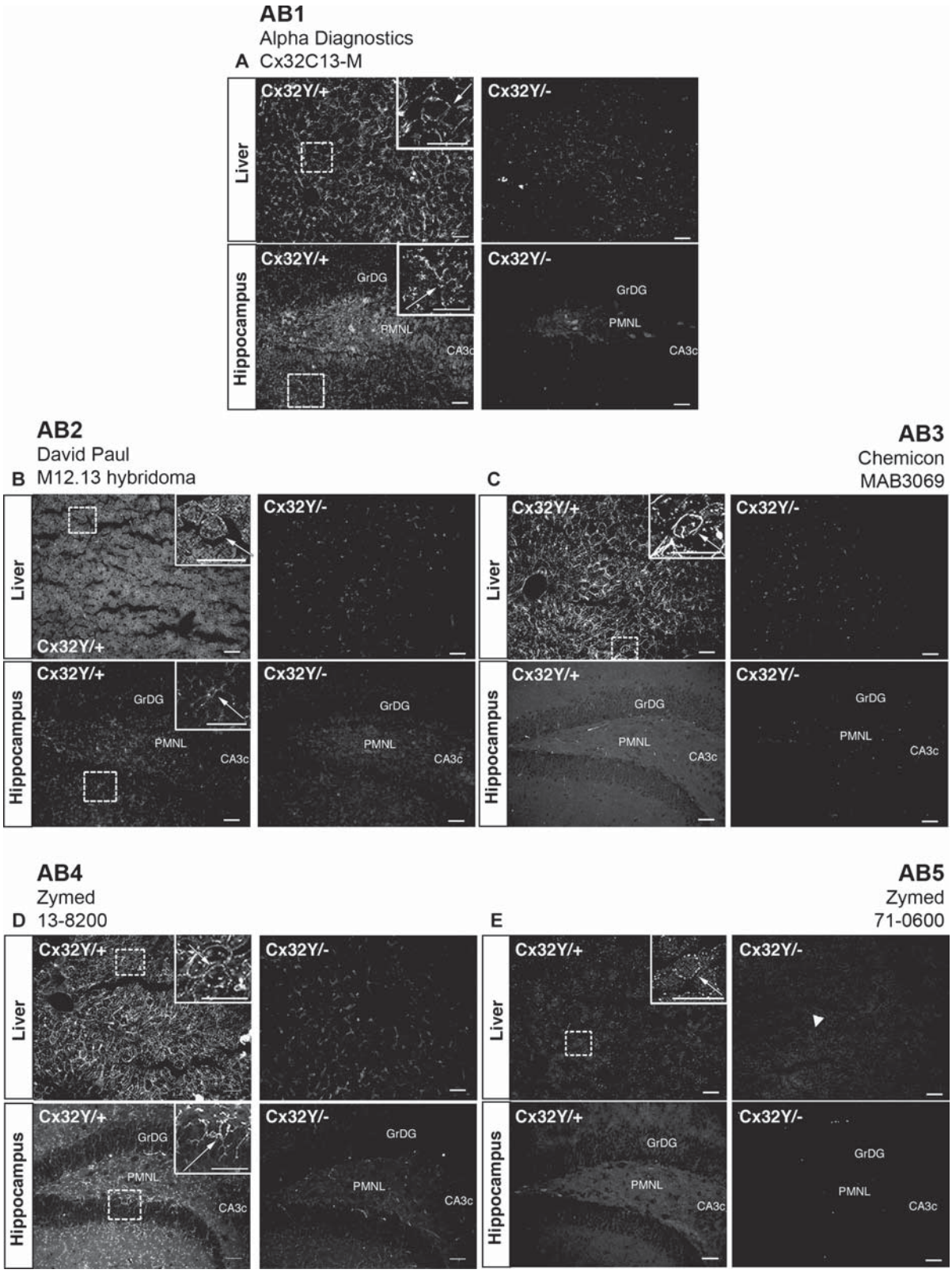

Figure 4. Specific immunofluorescent detection of Cx32 in both liver and brain using intracellular loop-directed antibodies. **(A–E)** All five antibodies directed against epitopes localizing to the Cx32 intracellular loop detected Cx32 at hepatocyte plasma membrane in $Cx32^{Y/+}$ liver tissue (*arrows, inset,* Liver), with minimal to no background reactivity in the $Cx32^{Y/-}$ controls with the exception of some low level background standing of hepatocyte plasma membrane with AB5 (*arrowhead,* Liver). **(A, B, D, E)** Four antibodies detected fixed protein in situ in $Cx32^{Y/+}$ mouse hippocampal sections with (D) AB4 providing the most robust signal. Hippocampal immunostaining was evident at the plasma membrane of cells with expected oligodendrocyte and/or oligodendrocyte precursor cell morphology (*arrows, inset,* Hippocampus). None of the antibodies exhibited significant cross-reactivity with $Cx32^{Y/-}$ brain tissue. GrDG, granule cell layer of the dentate gyrus; PMNL, polymorphonuclear layer of the dentate gyrus; CA3c, CA pyramidal cell field 3c of the hippocampus. Scale bars, 50 μm.

Cell Commun Adhes Downloaded from informahealthcare.com by University of Ottawa on 12/27/10
For personal use only.

RIGHTSLINK

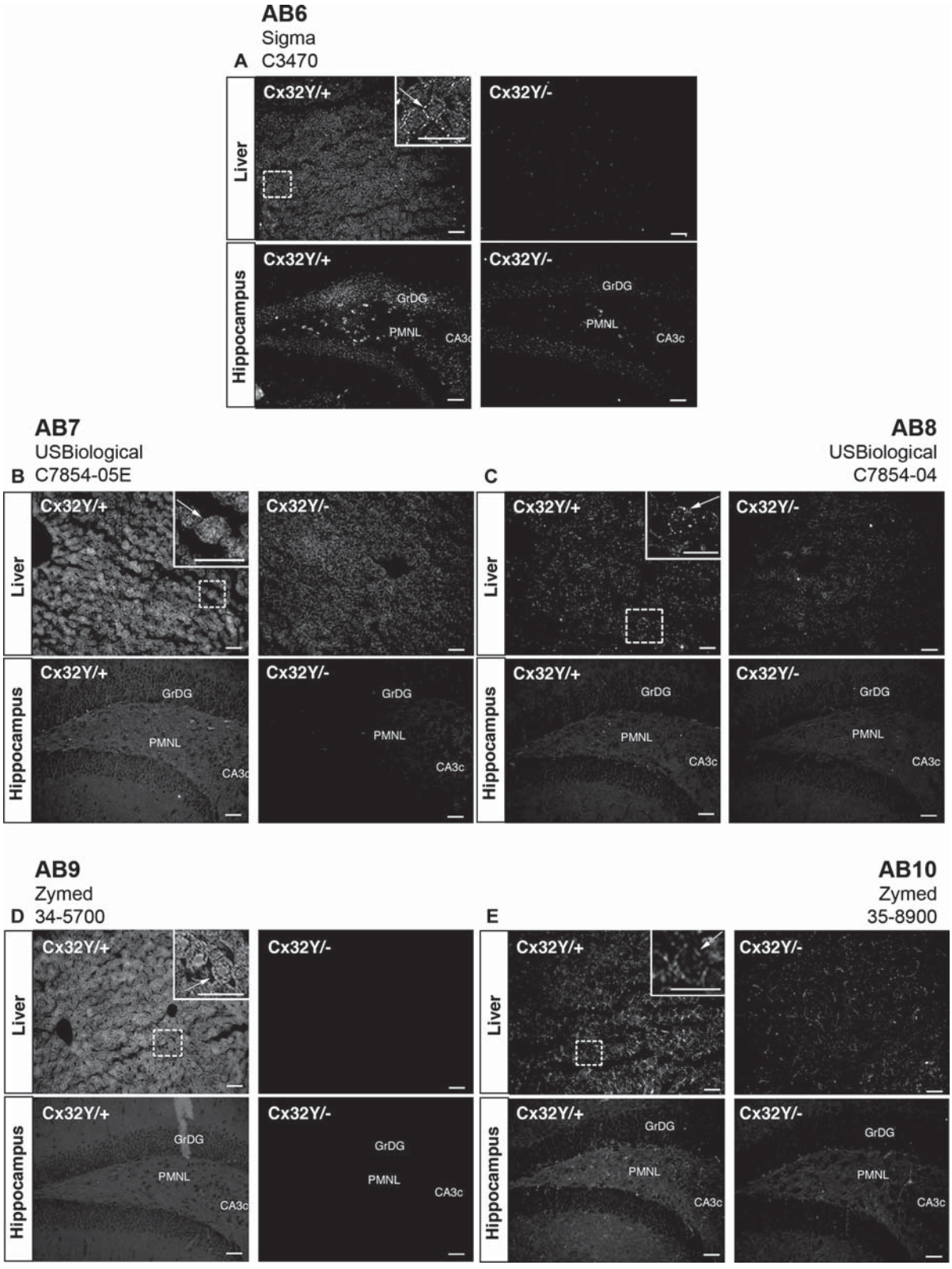

Figure 5. Specific immunofluorescent detection of Cx32 in liver but not brain using C-terminal tail-directed antibodies. **(A–E)** All five C-terminal antibodies detected Cx32 at hepatocyte plasma membrane in $Cx32^{Y/+}$ liver tissue (*arrows, inset,* Liver), with minimal to no background reactivity in the $Cx32^{Y/-}$ controls. No specific immunosignal was seen in the $Cx32^{Y/+}$ hippocampus under the specific fixation and processing conditions employed in this study. Abbreviations are as in Figure 4. Scale bars, 50 μm.

flotation gradients (Figure 7). In $Cx32^{Y/+}$ liver lysates, a single immunoreactive band was detected in the Triton X-100 insoluble pellet (Figure 7A, P) and fractions 4 to 6 (Figure 7A, fractions 4 to 6). This distribution reflected predominant localization to detergent-insoluble and detergent-soluble lipid raft and plasma membrane fractions

Cell Commun Adhes Downloaded from informahealthcare.com by University of Ottawa on 12/27/10
For personal use only.

RIGHTSLINK

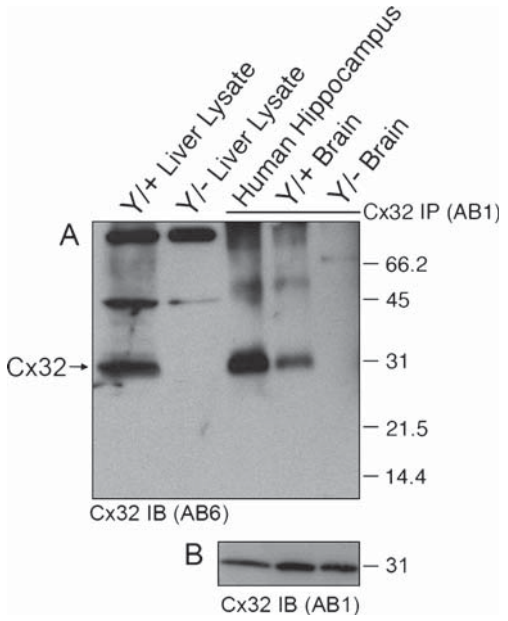

Figure 6. Brain-specific cross-reactivity is not observed following immunoprecipitation. **(A)** Cx32 lysates were purified from native RIPA lysates using monoclonal AB1, resolved under denaturing conditions by SDS-PAGE, and immunoblotted using polyclonal AB6. In the first two lanes WT ($Cx32^{Y/+}$) and null-mutant ($Cx32^{Y/-}$) liver lysates were subjected to Western analysis under reducing/denaturing conditions. The following three lanes represent human hippocampus and murine brain samples from WT ($Cx32^{Y/+}$) and null-mutant ($Cx32^{Y/-}$) controls immunoprecipitated with AB1 under native conditions before denaturing/reducing SDS-PAGE separation and immunoblotting with AB6. Specific immunoaffinity purification of Cx32 is observed under these conditions. **(B)** Standard Western analysis with aliquots of the same samples used in **(A)** reiterate the cross-reactivity observed when protein is first detected under reducing/denaturing conditions.

and possibly to mitochondria. No reactivity was detected in any of the fractions derived from control $Cx32^{Y/+}$ lysates (Figure 7B). Artifactual labeling was evident in $Cx32^{Y/+}$ and $Cx32^{Y/-}$ brain samples, as demonstrated in Figures 2 and 3, but with a detectable difference that could be used to distinguish specific Cx32 signal. Using a 15% SDS-PAGE gel (as compared to 12.5% gels presented in Figures 2 and 3), a reproducible difference in mobility was evident between brain and liver samples (Figure 7A, B). A single AB1-immunoreactive band was present in brain lysates (Figure 7A, Brain) migrating approximately 4 kDa faster than in liver lysates (Figure 7A, Liver). Following sucrose gradient fractionation of brain protein, this predominant species was evident in both $Cx32^{Y/+}$ and $Cx32^{Y/-}$ lysates (Figure 7C, D), but could be distinguished from a less abundant, higher molecular weight species (Figure 7C, *arrow*) migrating at approximately the same position as liver-derived Cx32 (compare Figure 7A and C). This band was absent from $Cx32^{Y/-}$ fractions (Figure 7D). The fractions enriched for the higher molecular weight Cx32-specific band (fractions 4, 5, and 6) were also enriched for the mitochondrial marker coxIV, both lipid-raft–associated protein markers caveolin-1 and flotillin-1, and the plasma membrane marker syntaxin-1 (Figure 7C). This subcellular fractionation matched that observed in liver (Figure 7A). Conversely, the fractions enriched for the smaller cross-reactive protein (fractions 7 to 10) in both $Cx32^{Y/+}$ and $Cx32^{Y/-}$ lysates (Figure 7C, D) were enriched for LAMP-1 (lysosomes) and golgin-97 (trans-Golgi network) (Figure 7C). Together, these data suggested that brain, but not liver, tissue expresses Cx32 at both plasma and perhaps mitochondrial membranes, as well as a cross-reactive protein enriched in the Golgi apparatus and lysosomes that is ~4 kDa smaller than Cx32.

Bioinformatic and Western Analyses Suggest That the Cross-Reactive Protein Is Not Another Connexin

We were surprised that antibodies directed at both the intracellular loop and the C-terminal region of Cx32 exhibited the same cross-reactivity. To address this, we used a bioinformatics approach to identify candidate proteins based on the pattern of cross-reactivity detected in Figures 2 and 3, the antigenic sites predicted in Table 2, and the tissue-specific expression pattern (Supplemental Methodology). This analysis predicted that the cross-reactive protein(s) would contain contiguous amino acid sequences, exposed under denaturing/reducing conditions, that share the EEVKRHKV and EGHGDPLH/GDPLHLEE epitopes (recognized by AB1 to AB4), but not the QQHIEKKM (recognized by Cx32-specific AB5) epitope found within the intracellular loop with Cx32, as well as at least three and likely four of the Cx32 C-terminal tail epitopes (recognized by AB6 to AB9), but no significant homology with the fifth predicted antigenic sequences (recognized by Cx32-specific AB10).

We used these assumptions to establish search criteria for other connexins with sufficient contiguous antigenic peptide sequences, tissue specificity, and electrophoretic mobility for potential cross-reactivity (Supplemental Methodology). One connexin (Cx30) met all criteria; two other connexins (Cx26 and Cx29) met some but not all parameters (Supplemental Methodology). However, direct assessment of lysates prepared from $Cx29^{-/-}$, $Cx29^{-/-}/Cx32^{Y/-}$, or $Cx30^{-/-}$ brain tissue provided conclusive evidence that the cross-reactive protein was still present in double- and single-null-mutant brain tissue and thus was not Cx29 or Cx30 (Figure 8A, B). Further, although Cx26 could be detected abundantly in wild-type mouse liver and, weakly in brain, Cx26 protein levels were substantively reduced in $Cx32^{Y/-}$ brain or liver tissue (Figure 8C) and thus Cx26 is unlikely to represent the cross reactive protein. This reduction in Cx26 protein levels in Cx32 null-mutant animals is consistent with previous studies (Nelles et al. 1996).

When placed in context with the subcellular localization evident in sucrose gradient fractionation (Figure 7), these data provided converging evidence to indicate that the cross-reactive protein is likely not another connexin but rather an immature (Golgi-localized) or partially degraded (lysosome-localized) subunit of a larger unidentified

Cell Commun Adhes Downloaded from informahealthcare.com by University of Ottawa on 12/27/10
For personal use only.

RIGHTSLINK

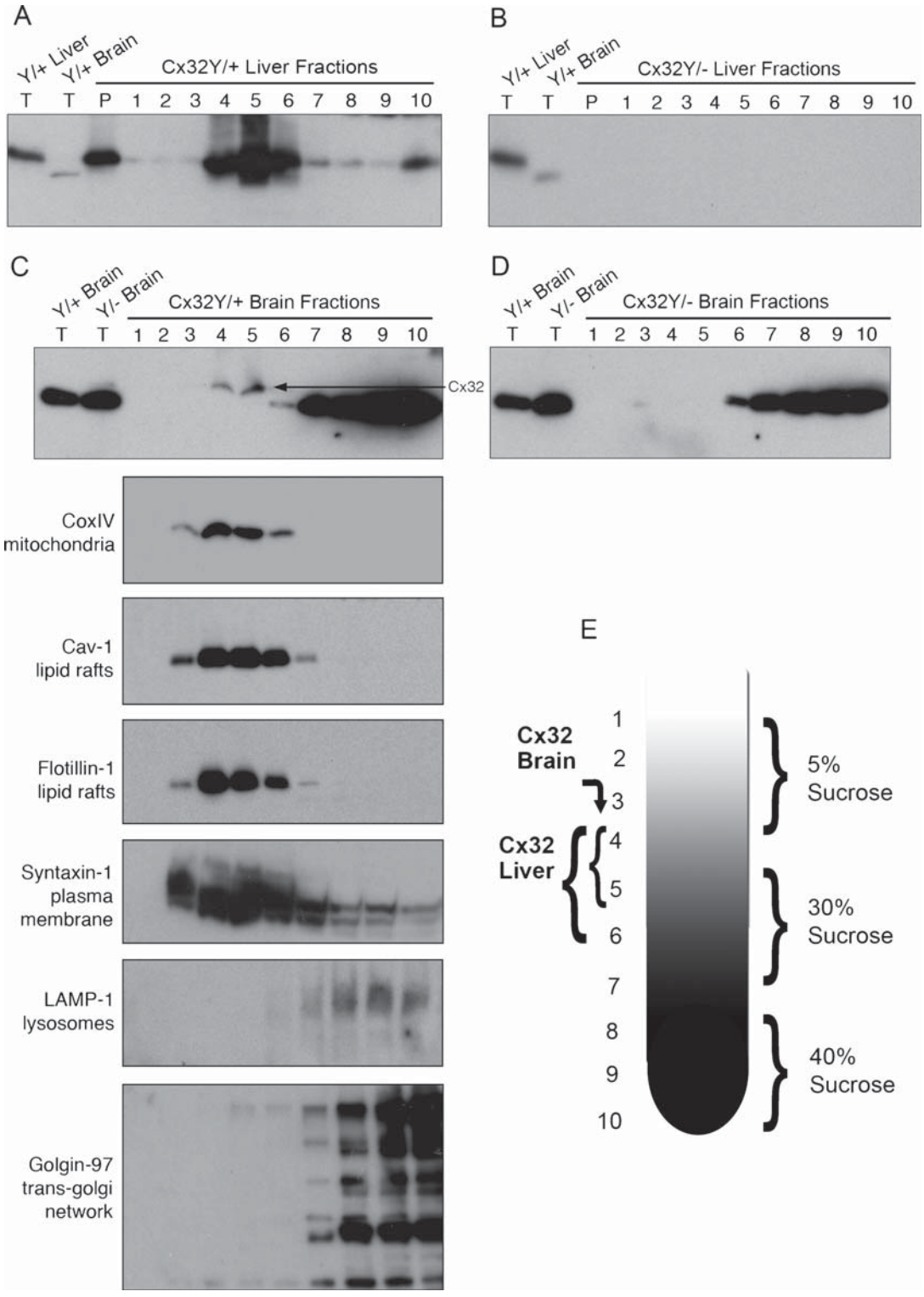

Figure 7. Sucrose gradient fractionation reveals that the brain-specific cross-reactive protein is approximately 4 kDa smaller than Cx32 and exhibits a distinct subcellular localization. **(A–D)** Total tissue lysates (T) or the Triton X-100–insoluble pellet (P) and (E) fractions 1 to 10 obtained through sucrose fractionation were immunoblotted under denaturing/reducing conditions using AB1. To achieve maximal separation, proteins were separated on 15% Tris-HCl polyacrylamide gels. Each lane contains 5 μg of protein. **(A)** Sucrose gradient fractions of $Cx32^{Y/+}$ liver are compared to total tissue lysates of $Cx32^{Y/+}$ liver or brain. Note the ~4-kDa size difference between the species predominating in $Cx32^{Y/+}$ liver compared to brain. **(B)** Sucrose gradient fractions of $Cx32^{Y/-}$ liver are compared to total tissue lysates of $Cx32^{Y/+}$ liver or brain. No signal was detected in $Cx32^{Y/-}$ control lysates. **(C)** Sucrose gradient fractions of $Cx32^{Y/+}$ brain are compared to total brain lysates prepared from $Cx32^{Y/+}$ and $Cx32^{Y/-}$ mice (*top panel*). Exposure times were extended from that shown in **A** and **B** to enable detection of endogenous Cx32 in fractions 4 and 5 (*arrow*), migrating 4 kDa higher than the cross-reactive protein that was present at higher abundance and enriched in fractions 6 to 10. Lower panels characterize each fraction using organelle-specific markers: mitochondria (coxIV), lipid rafts (caveolin-1 and flotillin-1), plasma membrane (syntaxin-1), lysosomes (LAMP-1), and the trans-Golgi

Cell Commun Adhes Downloaded from informahealthcare.com by University of Ottawa on 12/27/10
For personal use only.

RIGHTSLINK

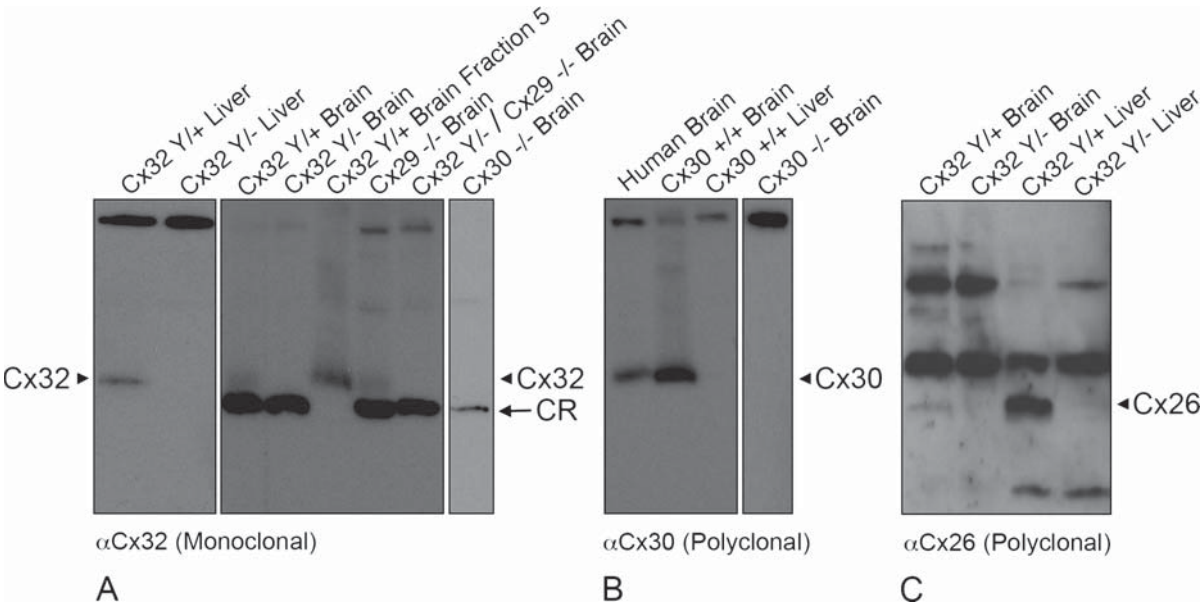

Figure 8. Cx32 antibodies do not cross-react with Cx26, Cx29, or Cx30 under denaturing/reducing conditions. **(A)** Liver and brain samples were prepared from wild-type ($Cx32^{Y/+}$), $Cx32^{Y/-}$, and $Cx29^{-/-}$. $Cx32^{Y/-}$/$Cx29^{-/-}$, or $Cx30^{-/-}$ null-mutant mice, separated on 15% Tris-HCl polyacrylamide gels, and immunoblotted for Cx32 using monoclonal AB1. To distinguish between the cross-reactive protein(s) and endogenous Cx32 in brain samples, fraction 5 lysate from sucrose gradient separations (see Figure 7) of WT ($Cx32^{Y/+}$) was included as a positive control. All brain samples, except WT brain fraction 5, exhibited the lower molecular weight cross-reactive band. Arrowheads indicate Cx32; arrows indicate the cross-reactive (CR) protein. **(B)** Immunoblotting of Cx30 in lysates prepared from human brain, wild-type mouse brain and liver, and $Cx30^{-/-}$ brain confirmed the presence of Cx30 in CNS tissue (*arrowhead*), absent from liver. Specificity was established using null-mutant controls. **(C)** Cx26 protein, present in $Cx32^{Y/+}$ brain and liver (*arrowhead*), was below detection levels in $Cx32^{Y/-}$ tissue.

protein complex with homologous epitopes unmasked only after protein denaturation and the reduction of disulfide bonds.

DISCUSSION

Here, we characterize a tissue-specific cross-reactivity with multiple commonly used Cx32 antibodies that impacts upon the interpretation of Western blots performed using CNS tissue. Although all 10 of the reagents tested reliably detect Cx32 in liver as expected, we found that 8 of these reagents cross-react with a CNS protein(s) that exhibits the same approximate electrophoretic mobility as Cx32. Comparing immunoblotting, immunofluorescence, and immunoprecipitation detection methods using $Cx32^{Y/+}$ and $Cx32^{Y/-}$ brain and liver tissue, we concluded that this artifactual cross-reactivity is only observed under denaturing/reducing conditions and does not complicate analyses that retain tertiary protein structure during initial immunodetection or immunopurification (i.e., in situ immunofluorescence or immunoprecipitation studies). These data indicate that cross-reactivity is likely the result of the unmasking of epitopes found in primary sequence not accessible in situ upon proper protein folding. Finally, two antibodies, polyclonal AB5 and monoclonal AB10 (Table 1), reliably detected Cx32 in Western analysis of brain tissue. These data are consistent with previous reports wherein AB5 and AB10 were shown to specifically recognize Cx32 in brain and liver (Nagy et al. 2003b), emphasizing the need for careful choice of antibody and methodology in the study of Cx32 in brain tissue.

To provide further insight into this tissue specificity, we identified three highly antigenic sites in the intracellular loop and five highly antigenic sites in the C-terminus of the Cx32 protein sequence. Based on these sites and the banding patterns produced by each of antibodies tested in Cx32 null-mutant tissue, we predicted that the primary sequence of the cross-reactive protein(s) would exhibit strict homology to six of these eight antigenic sites but would not contain the two unique epitopes that rendered AB5 and AB10 Cx32 specific. Moreover, the protein would be expressed in brain but not liver. Bioinformatic analyses encompassing all of these criteria identified only one protein, Cx30, with potential to cross-react under denaturing/reducing conditions. However, direct

Figure 7. (*Continued*)
network (Golgin-97). The fractionation of liver tissue exhibited the same pattern of organelle-specific immunoreactivity (data not shown). **(D)** Only the lower molecular weight cross-reactive band was present in sucrose gradient fractions prepared from $Cx32^{Y/-}$ mouse brain. **(E)** Schematic of the sucrose fractionation showing the gradients enriched for Cx32 in both brain and liver.

Cell Commun Adhes Downloaded from informahealthcare.com by University of Ottawa on 12/27/10
For personal use only.

RIGHTSLINK

assessment revealed that the brain-specific cross-reactive protein was still present in brain lysates prepared from not only Cx30$^{-/-}$ but also Cx29$^{-/-}$/Cx32$^{Y/-}$ mice and in the absence of Cx26. Further, sucrose gradient fractionation analyses revealed that the antigenically related cross-reactive protein(s) exhibited an ~4-kDa size difference, localized to different subcellular compartments, and was expressed at higher levels than Cx32 in brain tissue. Cx32 was found in fractions enriched for plasma membrane, lipid rafts, and mitochondrial markers; the brain-specific cross-reactive protein was found in fractions enriched for golgi and lysosome markers. This subcellular localization indicates that the cross-reactive protein is likely not a member of the connexin family.

In summary, this study addresses a CNS-specific problem in Cx32 antibody cross-reactivity that has been reported anecdotally but not analyzed directly. We show that, although all of the reagents tested are specific for Cx32 in liver, protein denaturation/reduction unmasks epitopes present in primary sequence of a CNS-specific protein, likely not another connexin, that exhibits the same approximate electrophoretic mobility as Cx32 and is present in mouse brain prepared from multiple connexin null-mutants. We show that this technical obstacle can be easily overcome by choice of antibody, careful size analysis, or exclusive use of immunoprecipitation to quantify changes in Cx32 protein expression. These data are presented with the intent of reducing the amount of time laboratories currently expend in validating changes in Cx32 expression in CNS.

Declaration of interest: The authors report no conflicts of interest. The authors alone are responsible for the content and writing of the paper.

REFERENCES

Altevogt BM, Kleopa KA, Postma FR, Scherer SS, Paul DL (2002). Connexin29 is uniquely distributed within myelinating glial cells of the central and peripheral nervous systems. *J Neurosci.* 22: 6458–6470.

Bruzzone R, White TW, Paul DL (1996). Connections with connexins: The molecular basis of direct intercellular signaling. *Eur J Biochem.* 238: 1–27.

Dermietzel R, Farooq M, Kessler JA, Althaus H, Hertzberg EL, Spray DC (1997) Oligodendrocytes express gap junction protein connexin32 and connexin45. *Glia.* 20: 101–114.

Goodenough DA, Paul DL (2003). Beyond the gap: Functions of unpaired connexon channels. *Nat Rev Mol Cell Biol.* 4: 285–294.

Goodenough DA, Paul DL, Jesaitis L (1988). Toplogical distrubution of two Connexin32 antigenic sites in intact and split rodent hepatocyte gap junctions. *J Cell Biol.* 107: 1817–1824.

Hertzberg EL (1985). Antibody probes in the study of gap junctional communication. *Annu Rev Physiol.* 47: 305–318.

Hopp TP, Woods KR (1981). Prediction of protein antigenic determinants from amino acid sequences. *Proc Natl Acad Sci U S A.* 78: 3824–3828.

Kolaskar AS, Tongaonkar PC (1990). A semi-empirical method for prediction of antigenic determinants on protein antigens. *FEBS Lett.* 276: 172–174.

Kyte J, Doolittle RF (1982). A simple method for displaying the hydropathic character of a protein. *J Mol Biol.* 157: 105–132.

Lambert JP, Mitchell L, Rudner A, Baetz K, Figeys D (2009). A novel proteomics approach for the discovery of chromatin-associated protein networks. *Mol Cell Proteomics.* 8: 870–882.

Li J, Hertzberg EL, Nagy JI (1997). Connexin32 in oliogdendrocytes and association with myelinated fibers in mouse and rat brain. *J Comp Neurol.* 379: 571–591.

Luque-Garcia JL, Zhou G, Spellman DS, Sun TT, Neubert TA (2008). Analysis of electroblotted proteins by mass spectrometry: Protein identification after Western blotting. Mol Cell Proteomics. 7: 308–314.

Melanson-Drapeau L, Beyko S, Davé S, Hebb ALO, Franks DJ, Sellito C, Paul DL, Bennett SAL (2003). Oligodendrocyte progenitor enrichment in the connexin32 null-mutant mouse. *J Neurosci.* 23: 1759–1768.

Nagy JI, Dudek FE, Rash JE (2004). Update on connexins and gap junctions in neurons and glia in the mammalian nervous system. *Brain Res Brain Res Rev.* 47: 191–215.

Nagy JI, Ionescu AV, Lynn BD, Rash JE (2003a). Connexin29 and connexin32 at oligodendrocyte and astrocyte gap junctions and in myelin of the mouse central nervous system. *J Comp Neurol.* 464: 356–370.

Nagy JI, Ionescu AV, Lynn BD, Rash JE (2003b). Coupling of astrocyte connexins Cx26, Cx30, Cx43 to oligodendrocyte Cx29, Cx32, Cx47: Implications from normal and connexin32 knockout mice. *Glia.* 44: 205–218.

Nakase T, Naus CC (2004). Gap junctions and neurological disorders of the central nervous system. *Biochim Biophys Acta.* 1662: 149–158.

Nelles E, Buetzler C, Jung D, Temme A, Gabriel HD, Dahl U, Traub O, Stuempel F, Jungermann K, Zielasek J, Toyka KV, Dermietzel R, Willecke K (1996). Defective propagation of signals generated by sympathetic nerve stimulation in the liver of connexin32-deficient mice. *Proc Natl Acad Sci USA.* 93: 9565–9570.

Paul DL (1986). Molecular cloning of cDNA for rat liver gap junction protein. *J Cell Biol.* 103: 123–134.

Rouach N, Avignone E, Meme W, Koulakoff A, Venance L, Blomstrand F, Giaume C (2002). Gap junctions and connexin expression in the normal and pathological central nervous system. *Biol Cell.* 94: 457–475.

Scherer SS, Deschenes SM, Xu Y, Grinspan JB, Fischbeck KH, Paul DL (1995). Connexin32 is a myelin-related protein in the PNS and CNS. *J Neurosci.* 15: 8281–8294.

Sohl G, Maxeiner S, Willecke K (2005). Expression and functions of neuronal gap junctions. *Nat Rev Neurosci.* 6: 191–200.

Teubner B, Michel V, Pesch J, Lautermann J, Cohen-Salmon M, Sohl G, Jahnke K, Winterhager E, Herberhold C, Hardelin JP, Petit C, Willecke K (2003). Connexin30 (Gjb6)-deficiency causes severe hearing impairment and lack of endocochlear potential. *Hum Mol Genet.* 12: 13–21.

Traub O, Janssen-Timmen U, Druge PM, Dermietzel R, Willecke K (1982). Immunological properties of gap junction protein from mouse liver. *J Cell Biochem.* 19: 27–44.

Traub O, Willecke K (1982). Cross reaction of antibodies against liver gap junction protein (26K) with lens fiber junction protein (MIP) suggests structural homology between these tissue specific gene products. *Biochem Biophys Res Commun.* 109: 895–901.

Cell Commun Adhes Downloaded from informahealthcare.com by University of Ottawa on 12/27/10
For personal use only.

RIGHTSLINK

APPENDIX

Supplemental Methodology: Bioinformatics

Three potential antigenic sequences were detected within the intracellular loop of Cx32 (Figure 2A to E, Table 2). Two of these sequences were present in the peptide used to generate AB1. All three sequences were present in AB2 and AB3. Because AB1, AB2, and AB3 are monoclonal antibodies and generated identical banding patterns (Figure 2A to C), it is likely that they recognize the same epitope, either the EEVKRHKV or the EGHGDPLH/GDPLHLEE antigenic sequence, located towards the C-terminus of the intracellular loop encompassed by the peptides used to generate AB1 (Table 2). Although the exact peptide sequence used to generate AB4 and AB5 was not disclosed by the manufacturer, both antibodies were distinguished from AB1 to AB3 by a species variation in the doublet detected in human samples (Figure 2D). Based on this difference, we hypothesized that they likely detect one of the two potential epitope variants (EGHGDPLH/GDPLHLEE) (Table 2). Only polyclonal AB5 demonstrated specificity and thus we hypothesized that it recognizes the only antigenic sequence that does not overlap with AB1 (i.e., QQHIEKKM) located towards the N-terminus of the intracellular loop (Table 2). This analysis predicted that the cross-reactive protein would contain contiguous amino acid sequences, exposed under denaturing/reducing conditions, that share the EEVKRHKV and EGHGDPLH/GDPLHLEE but not the QQHIEKKM epitopes with Cx32.

In the C-terminal tail of Cx32, five potentially antigenic sequences were detected (Figure 3A to E, Table 2). Polyclonal AB6 (Figure 3A) was directed against a known sequence that encompassed the most distal C-terminal tail antigen (GLAEKSDR, Table 2). Polyclonal AB7 generated a pattern distinct from all of the other reagents and thus likely recognizes epitope(s) distinct from AB6 (Figure 3B). AB8 and AB9 detected a doublet in human brain samples and thus likely recognize the same

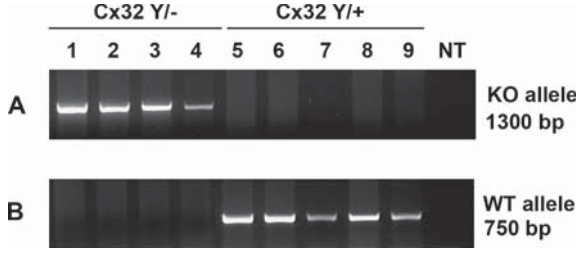

Supplemental Figure 1. Genotyping for Cx32 WT or null-mutant KO allele. All mice were genotyped at both the time of weaning and time of sacrifice for (**A**) a 1300-bp KO amplicon and (**B**) a 750-bp WT amplicon. Representative genotyping from four null-mutant mice ($Cx32^{Y/-}$) and five WT mice ($Cx32^{Y/+}$) used in this study is shown. NT represents no template control, confirming lack of reagent contamination.

species-specific antigenic sequences (Figure 3C, D). AB10 was Cx32 specific and, as a monoclonal antibody, is raised against a single epitope (Figure 3E). Based on this pattern, we predicted that the cross-reactive protein would contain, in addition to the epitopes recognized by the intracellular loop antibodies, contiguous sequences in primary sequence homologous to at least three and likely four of the Cx32 C-terminal tail epitopes but no significant homology with the fifth predicted antigenic sequences (recognized by Cx32-specific AB10).

Only Cx30 met these criteria. The intracellular loop EEVKRHKV epitopes exhibited a significant alignment score of 62% whereas alignment of the EGHGDPLH/GDPLHLEE antigenic sequences met the minimum number of adjacent amino acids required to raise an antigenic response (contiguous alignment score of 25). Further, as predicated, the QQHIEKKM epitope was not found in the Cx30 primary sequence (alignment score of 12%). Four of the five Cx32 C-terminal tail epitopes produced significant alignment scores of 25 to 62. The fifth epitope NPPSRKGS did not exhibit any significant alignment in contiguous sequence (≤12%). Despite this potential homology, stringent testing with null-mutant controls provided conclusive evidence that Cx32 antibodies do not cross-react with Cx30 (Figure 8).

Copyright © ARVO (unless otherwise stated). For non-commercial use only. Terms of use exhibited. Any copy and print will be for personal use only. Unauthorized distribution is prohibited.